A spectroscopic study of IRAS F10214 + 4724

Mon. Not. R. Astron. Soc. **298,** 321–331 (1998)

A spectroscopic study of IRAS F10214 + 4724

Stephen Serjeant,[1,2] Steve Rawlings,[2] Mark Lacy,[2] Richard G. McMahon,[3] Andy Lawrence,[4] Michael Rowan-Robinson[1] and Matt Mountain[5]

[1]*Astrophysics Group, Imperial College London, Blackett Laboratory, Prince Consort Road, London SW7 2BZ*
[2]*Astrophysics, Department of Physics, Keble Road, Oxford OX1 3RH*
[3]*Institute of Astronomy, The Observatories, Madingley Road, Cambridge CB3 0HA*
[4]*Institute for Astronomy, University of Edinburgh, Royal Observatory, Blackford Hill, Edinburgh EH9 3HJ*
[5]*Gemini 8-m Telescopes Project, 950 N. Cherry Avenue, Tucson, AZ 85726, USA*

Accepted 1998 February 11. Received 1998 February 11; in original form 1996 July 9

ABSTRACT

The $z = 2.286$ *IRAS* galaxy F10214 + 4724 remains one of the most luminous galaxies in the Universe, despite its gravitational lens magnification. We present optical and near-infrared spectra of F10214 + 4724, with clear evidence for three distinct components: lines of width $\sim$1000 km s^{-1} from a Seyfert 2 nucleus; $\lesssim$ 200 km s^{-1} lines which are likely to be associated with star formation; and a broad ($\sim$4000 km s^{-1}) C III] 1909-Å emission line which is blueshifted by $\sim$1000 km s^{-1} with respect to the Seyfert 2 lines. Our study of the Seyfert 2 component leads to several new results. (i) From the double-peaked structure in the Lyα line, and the lack of Lyβ, we argue that the Lyα photons have emerged through a neutral column of $N_{\rm H} \sim 2.5 \times 10^{25}$ m^{-2}, possibly located within the AGN narrow-line region, as proposed for several high-redshift radio galaxies. (ii) The resonant O VI 1032, 1036-Å doublet (previously identified as Lyβ) is in an optically thick (1:1) ratio. At face value this implies an extreme density ($n_{\rm e} \sim 10^{17}$ m^{-3}) more typical of broad-line region clouds. However, we attribute this instead to the damping wings of Lyβ from the resonant absorption. (iii) A tentative detection of He II 1086 suggests little extinction in the rest frame ultraviolet.

Key words: galaxies: active – galaxies: formation – galaxies: individual: FSC 10214 + 4724 – galaxies: starburst – gravitational lensing – infrared: galaxies.

1 INTRODUCTION

The $z = 2.286$ *IRAS* galaxy FSC 10214 + 4724 (hereafter F10214 + 4724) is one of the most apparently luminous objects in the Universe, and its discovery (Rowan-Robinson et al. 1991) led to much speculation about its possible status as a protogalaxy. This speculation was based on the extreme bolometric luminosity of the object (Rowan-Robinson et al. 1991), and more specifically on the huge gas mass and star formation rate inferred from the submm molecular line and continuum detections (e.g. Solomon, Downes & Radford 1992; Rowan-Robinson et al. 1993).

This speculation was dampened by a series of papers which proved that F10214 + 4724 is being gravitationally lensed and, at all wavebands, is intrinsically in order of magnitude or more dimmer than it first appeared. Although a lensing bias was suspected by a number of authors (e.g. Elston et al. 1994; Trentham 1995), the first direct empirical evidence of strong gravitational lensing was provided by a deep near-infrared image (Matthews et al. 1994), which revealed an arc-like structure centred on a galaxy close to the line of sight to F10214 + 4724. Several sets of authors published lensing interpretations (Broadhurst & Lehár 1995; Graham & Liu 1995; Serjeant et al. 1995), which were confirmed by the appearance of the *HST* image obtained by Eisenhardt et al. (1996): this image contained highly elliptical, high-surface-brightness features characteristic of strong lensing, as well as a clear counterimage. These papers also attempted to constrain the redshift of the system responsible for the gravitational lensing, our contribution (Serjeant et al. 1995) being spectroscopy of two galaxies projected $\approx$1 and $\approx$3 arcsec from F10214 + 4724. This work revealed tentative 4000-Å breaks at $z \simeq 0.90$ in both galaxies, later confirmed using fundamental plane arguments in *HST* imaging (Eisenhardt et al. 1996), and also tentatively supported by a weak absorption line at $z = 0.893$ in the F10214 + 4724 spectroscopy of Goodrich et al. (1996). The *HST* *R*-band image of F10214 + 4724 implies magnifications of $\sim$100 (Eisenhardt et al. 1996) in this waveband, but it now seems likely that differential flux magnification causes lower magnification factors for the more extended structure, as argued by several authors.

Gravitational lensing appeared to offer a compelling explanation for the extreme luminosity of F10214 + 4724 (e.g. Broadhurst & Lehár 1995). As a result, the *IRAS* galaxy is no longer so extreme in its properties: indeed, in many respects it resembles local ultraluminous infrared galaxies and Seyfert 2 galaxies. Nevertheless, both Downes, Solomon & Radford (1995) and Green &

Rowan-Robinson (1996) argue for a bolometric magnification factor of $\lesssim 10$ using arguments based on minimum blackbody sizes. F10214 + 4724 remains one of the most intrinsically luminous objects in the Universe. The importance in this object still lies in studying whether high-z hyperluminous activity, such as that seen in F10214 + 4724, differs in all but scale from local objects, and in determining the relative contributions of the starburst and AGN components (Lawrence et al. 1993, 1994; Elston et al. 1994; Soifer et al. 1995; Goodrich et al. 1996; Kroker et al. 1996; Hughes, Dunlop & Rawlings 1997).

Prior to making the observations reported in this paper there had been no direct evidence for the presence of an embedded broad-line (e.g., Seyfert 1 or quasar) nucleus in F10214 + 4724, although high (≈20 per cent) rest frame ultraviolet (UV) polarization (Lawrence et al. 1993; Jannuzi et al. 1994) suggested that one was present. This situation changed with the deep spectropolarimetry of Goodrich et al. (1996) showing clear broad lines in polarized light. This extended the close spectral similarities between F10214 + 4724 and Seyfert 2 galaxies, specifically NGC 1068, which was first remarked on by Elston et al. (1994).

Prior to our observations there had also been no reported detection of the narrow ($\lesssim 200$ km s^{-1}) emission lines expected from any star-forming activity in F10214 + 4724. A star-forming component is expected if the analogy with NGC 1068 is to be complete. This situation also changed during the preparation of this paper. Using a novel imaging near-infrared spectrometer, Kroker et al. (1996) presented evidence for spatially extended narrow Hα emission, just as expected if the Seyfert 2 nucleus of F10214 + 4724 is accompanied by a circumnuclear starburst.

In this paper we present, analyse and interpret optical and near-infrared spectroscopy of F10214 + 4724. The details of data acquisition and analysis are given in Section 2. In Section 3 we compare our results with previous and contemporaneous spectroscopic studies of F10214 + 4724. In Section 4 we interpret the data on the Seyfert 2 emission-line region, including a discussion of optical depth effects on the resonance lines, and some modelling of the spectrum using the photoionization code CLOUDY (e.g. Ferland 1993, 1996). In this section we reach conclusions about the Seyfert 2 properties of F10214 + 4724 which differ significantly from those reached by previous studies. In Section 5 we interpret the data on

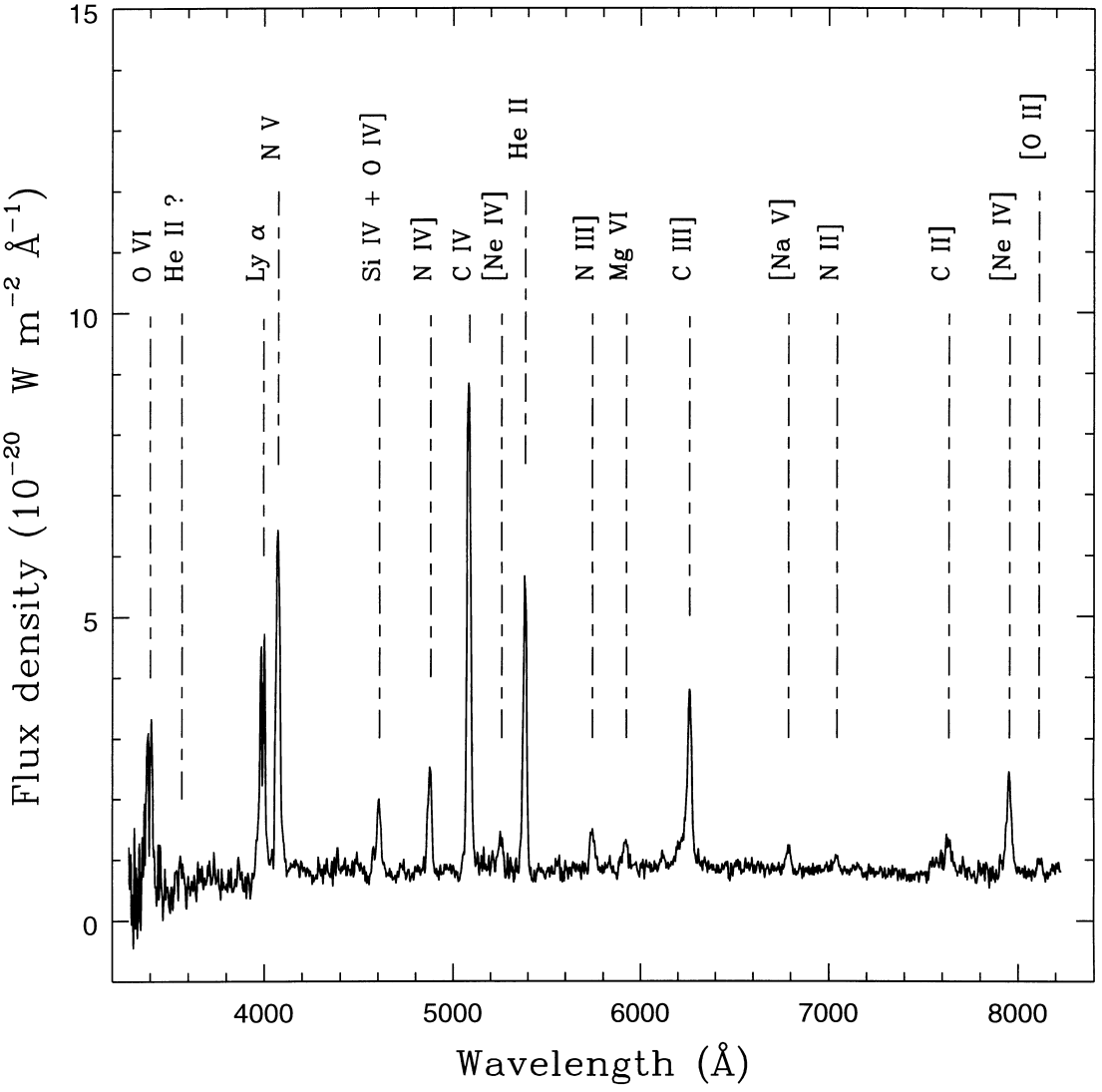

Figure 1. WHT spectrum of F10214 + 4724. The spectrum was extracted from a full-width, zero-intensity aperture, thereby ensuring accurate spectrophotometry. This also included some light from a nearby companion object, particularly redward of ≈7500 Å, as discussed by Serjeant et al. (1995). The emission lines are marked with their identifications.

the region responsible for the narrow ($\lesssim 200$ km s^{-1}) Hα line seen in our near-infrared spectrum: this feature is likely to be a signature of star formation. In Section 6 we make some concluding remarks on the nature of F10214 + 4724. Further data on galaxies foreground to F10214 + 4724 are given in Appendix A, and our attempts at identifying the weak emission line at 2067 Å are discussed in Appendix B.

2 DATA ACQUISITION AND ANALYSIS

2.1 Optical spectroscopy

We observed F10214 + 4724 on the nights of 1995 January 28 and 30 with the ISIS spectrograph on the William Herschel Telescope (WHT), taking advantage of 0.7-arcsec seeing. We refer the reader to Serjeant et al. (1995) for full details of these observations. The spectrophotometry is in good agreement with the continuum measurements tabulated by Rowan-Robinson et al. (1993) as well as (accounting for slit losses) the line parameters of Goodrich et al. (1996). There are significant disagreements between our measurements and those tabulated by Elston et al. (1994) – their line fluxes are typically larger by a factor of $\sim$2 – but these disagreements can plausibly be attributed to imperfect correction for the non-photometric observing conditions experienced by Elston et al. Neither the continuum nor any of the emission lines are resolved spatially (with $\approx$0.35-arcsec pixels); limits on the extended line emission are discussed by Serjeant et al. (1995).

2.2 Near-infrared spectroscopy

We observed F10214 + 4724 on two occasions with the short (150-mm) camera and 3-arcsec (single pixel) slit of the 62×58 InSb CGS4 array (Mountain et al. 1990) on the UKIRT. The slit was aligned at a position angle of 90°. The first of these observations, on 1992 February 5, used the 75 line mm^{-1} grating to obtain a first-order spectrum centred near 1.6 μm; a series of 30-s exposures were arranged in sets of four, shifted by 0, 0.5, 1 and 1.5 in wavelength – this provided Nyquist sampling and ensured that a given wavelength was sampled by two pixels. The standard 'ABBA' nodding pattern with a nod of 24 arcsec (eight detector rows) was used. The total exposure time was $9 \times 4 \times 2 \times 30$ s for each point in the 126-pixel spectrum. The second observation, on 1992 March 23, employed the 150 line mm^{-1} grating to obtain a second-order spectrum centred near 2.16 μm. The nod in this case was 30 arcsec (10 rows), and the total exposure time $10 \times 4 \times 2 \times 40$ s per point. Spectra were wavelength-calibrated using xenon/argon lamps and night-sky hydroxyl lines, flux-calibrated using HD 105601, and the positive and negative channels were extracted from their respective 3-arcsec-wide rows. The wavelength calibration is accurate to $\sim$0.003 μm in H and 0.001 μm in K, and the spectral resolving powers were 250 at H and 1400 at K.

3 RESULTS AND COMPARISON WITH OTHER SPECTROSCOPY

3.1 Optical spectroscopy

Fig. 1 shows our WHT optical spectrum of F10214 + 4724; line fluxes, widths and redshifts are tabulated in Table 1. Deeper spectra covering the region above 3900 Å have been presented by Soifer et al. (1995) and Goodrich et al. (1996), and an MMT spectrum, comparable in sensitivity and wavelength range to our data, is presented by Close et al. (1995); see also Rowan-Robinson et al. (1991) for the discovery spectrum. The velocity profiles of all the emission lines except Lyα are, with FWHMs around 1000 km s^{-1}, extremely similar. These linewidths are small compared to quasar

Table 1. Measurements from the WHT spectrum of F10214 + 4724.

Line Line	Position /Å	Redshift	EW / Å	Line flux /10^{-19} W m^{-2}	Accuracy	Line width kms^{-1}	Comments
O VI 1031.9	3388	2.283	60	4.5	30%	1200–1600	
O VI 1037.6	3408	2.284	60	4.3	30%	500–1200	
CIII? 1175.7	3866	2.288	6	0.4	60%		
Lyα 1215.7	3987	2.279	45	5.3	30%	0–900	two Gaussian
Lyα 1215.7	4002	2.292	40	4.7	30%	0–600	fit poor
N V 1240.1	4074	2.285	130.0	14	20%	1500–1700	doublet marginally resolved
CII 1335.3	4390	2.288	4	0.3	60%		
Si IV 1393.7	4577	2.284	8	0.7	50%		
O IV] 1402.5	4607	2.285	40	3.3	30%	1300–1500	blended with Si IV 1402.8
N IV] 1486.5	4879	2.282	45	4.0	25%	1250–1450	
C IV 1549.0	5087	2.284	150	19.0	20%	900–1200	
[Ne IV] 1602.0	5257	2.282	10	1.1	40%	1000-1200	
HeII 1640.5	5385	2.283	100	10.0	20%	800-1150	
N III] 1750	5743	2.282	20	2.0	30%	1200-1350	
Mg VI 1806	5924	2.280	15	1.5	40%	1200-1350	
Al III 1857.4?	6104	2.286	5	0.5	60%		Unidentified red wing
C III] 1908.7 narrow	6267	2.283	60	6.5	30%	800-1000	
C III] 1908.7 broad	6244	2.271	35	5.3	40%	≈3700	
[Na V] 2068	6791	2.265	10	1.2	40%	1000-1150	see text
N II] 2142.8	7045	2.287	8	0.8	50%	950-1100	blend with Si VII 2148 ?
C II] 2326.3	7638	2.284	30	3.0	40%	≈1500	blend with OIV 2321 ?
[Ne IV] 2422.0	7955	2.284	40	5.2	30%	900-1050	
[O II] 2470.3	8115	2.285	12	0.8	30%	1000-1150	
[O III] 4959	16279	2.283	280	23.4	30%	< 1300	
[O III] 5007	16453	2.286	580	49.8	30%	< 1300	
[N II] 6584	21634	2.286	14	6.6	30%	<200	
Hα	21564	2.286	12	5.5	30%	<200	
Hα+[N II] broad	21585	~ 2.28	83	38.3	20%	~ 1800	not deblended

Notes: Errors on the line fluxes represent $\sim$90 per cent confidence intervals expressed as a percentage of the best line-flux estimate; for the strongest lines these are dominated by roughly equal contributions from uncertainties in fixing the local continuum level, and in the absolute flux calibration. Linewidths were estimated from the FWHM of the best Gaussian fit to each line; for the restframe UV lines, the range lower value assumes that the line-emitting region fills the 2-arcsec WHT slit, and the higher value that is broadened only by the seeing.

broad lines, but large compared to AGN narrow lines, which are typically a few hundred km s^{-1} (e.g. Nelson & Whittle 1996).

The accuracy of our wavelength calibration means that the identification of the bright doublet in the far-blue with O VI is secure, and we are forced to conclude that Close et al. (1995) were mistaken in preferring Lyβ as the identification for this feature. This is probably the most clearly resolved example of the O VI doublet (see, e.g., Kriss et al. 1992a,b and Laor et al. 1994), a factor we will exploit in Section 4. Above 3900 Å, comparison with the published spectra shows that all the labelled feature are real. The identification of the (rest frame) 2470-Å feature, which is also seen in NGC 1068, is new, but probably uncontroversial. The identification of the line at ≈1805 Å is more uncertain: we have followed Lacy & Rawlings (1994) by identifying it with Mg VI, a line present in the CLOUDY models discussed in Section 4.2. A strong line at this wavelength is also seen in NGC 1068 (Snijders, Netzer & Boksenberg 1986). We prefer the Mg VI identification to either the Si II 1814.0-Å multiplet or the [Ne III] 1814.6-Å line: these were suggested as possible identifications by Snidjers et al., and adopted for F10214 + 4724 by Soifer et al. (1995) and Close et al. (1995). Note that the ionization potential of Mg^{5+} is 141.2 eV, and is thus even more extreme than the 113.9 eV required to produce O^{5+}.

This leaves one unidentified line at a rest frame wavelength of 2067 Å. This line is also seen in the *HST* spectrum of NGC 1068 (Antonucci, Hurt & Miller 1994), where it lies in a region confused by underlying Fe II multiplets (see also Wills, Netzer & Wills 1980 for a discussion of a 2080-Å feature in the spectra of quasars), but in F10214 + 4724 it is clearly a distinct narrow feature. Our attempts at identifying this line are discussed in Appendix B.

The broad asymmetric base to the C III]1909 line is shown in more detail in Fig. 3. This broad base is independently present (though marginally) in the spectra taken on both nights. The data are reproduced by the sum of two Gaussian components with a broad (∼4000 km s^{-1}) component, blueshifted by about 1000 km s^{-1} relative to a component with a similar FWHM (i.e., ≈1000 km s^{-1}) to the other optical lines. Although lines of Si III] are expected to be present at some level in the blue wing of C III]1909 (see Fig. 2), we were unable to obtain as good a fit using a superposition of ≈1000 km s^{-1} lines (Fig. 2). This implies that the previous detection of hint of a broad C III]1909 line is integrated light (Goodrich et al. 1996) is not attributable solely to the neighbouring narrow emission lines.

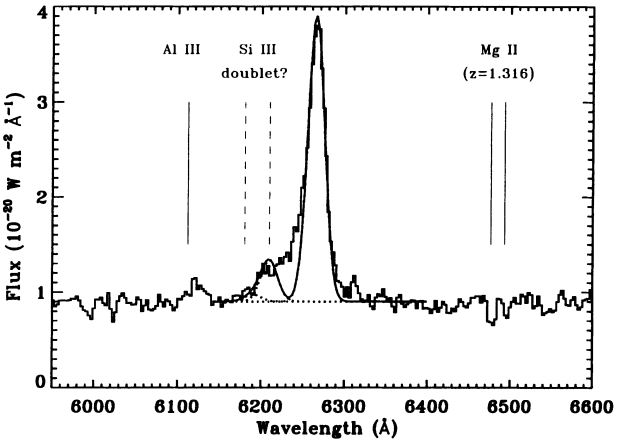

Figure 2. C III] line modelled as a narrow line and narrow Si III doublet. The individual model components are plotted as dotted lines, and the sum as a full line. Clearly, this makes an extremely poor fit to the data. The positions of the Al III emission line and the $z = 1.361$ Mg II absorber are also marked.

There is also an apparent blue wing to the C II]2326 line, but this feature is sensitive to the correction for the atmospheric A band. The lack of broad components to other lines may be explainable by a combination of scattering albedo and reddening towards the scattering surface [or between the broad-line region (BLR) and the scatterers, or within the scattering region itself]; also, lower signal-to-noise ratios may mask broad features in the Lyα and N V region (Fig. 4).

The Lyα line has a number of unusual properties which have been noted by other authors. First, it is weak relative to the other ultraviolet emission lines, e.g., N V. This appears to reflect anomalously weak Lyα emission: ignoring Lyα, both NGC 1068 (e.g. Snidjers et al. 1986; Kriss et al. 1992b) and the *IRAS*-detected Seyfert 2 galaxy NGC 3393 (Diaz, Prieto & Wamsteker 1988) have ultraviolet spectra similar to that of F10214 + 4724. Secondly, the Lyα line is double-peaked; this has been interpreted as requiring 'self-absorption' (Soifer et al. 1995; Close et al. 1995). We will discuss these points further in Section 4.

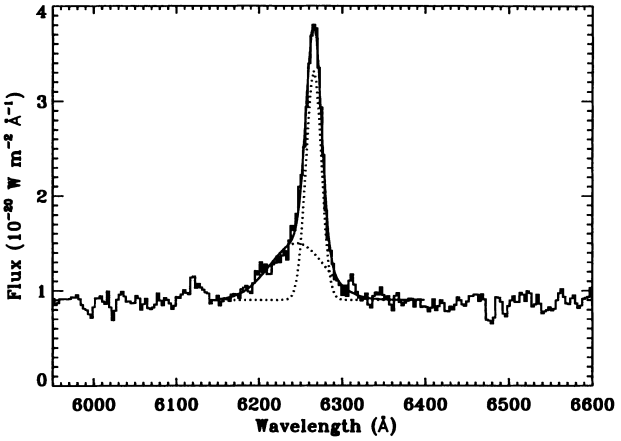

Figure 3. C III] line modelled as two Gaussians.

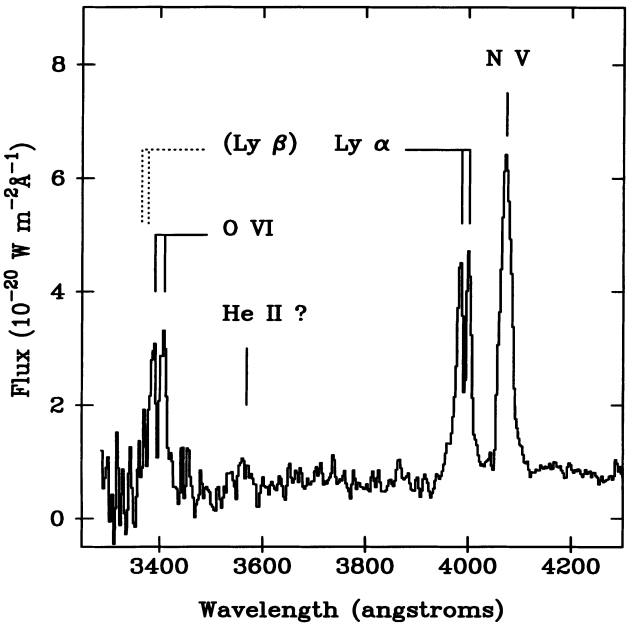

Figure 4. Expanded UV spectrum of F10214 + 4724. Positions of major emission lines are marked; also shown are the predicted positions of Lyβ associated with the observed Lyα.

The continuum depression shortward of Lyα is within the range, though at the upper limit observed in quasars at similar redshifts (e.g. Warren, Hewitt & Osmer 1994), consistent with the expected lack of a QSO proximity effect (e.g. Giallongo et al. 1996, and references therein). The He II 1086 line may be marginally detected. We confirm the presence of a Mg II 2800 absorption doublet at $z = 1.316$ (see Fig. 2), but have insufficient sensitivity to confirm the weaker $z = 0.892$ doublet tentatively identified by Goodrich et al. (1996).

3.2 Near-infrared spectroscopy

Our *H*-band spectrum of F10214 + 4724 is shown in Fig. 5, and our *K*-band spectrum in Fig. 6. Other near-inrared spectroscopy of F10214 + 4724 has been published by Elston et al. (1994), Iwamuro et al. (1995), Soifer et al. (1995) and Kroker et al. (1996).

We obtain an approximate lower limit on the [O III]4959 + 5007 to Hβ ratio of 10. Iwamuro et al. (1995) claim a tentative detection of Hβ with an O III to Hβ ratio of 27, although the Hβ is a factor of 3 brighter than the upper limit quoted by Elston et al. (1994). Iwamuro et al. used the OH airglow suppressor spectrograph on the University of Hawaii 2.2-m telescope, so their detection should be less prone to difficulties in sky subtraction. However, it is not clear how imperfect sky subtraction could lead to an underestimate of the Hβ flux without a corresponding null detection of the [O III]4959, 5007-Å doublet, since the sky lines are if anything stronger near the [O III] lines, and the relative variations of the sky lines are typically $\leq$10 per cent (Ramsay, Mountain & Geballe 1992); there are also no strong atmospheric absorption lines in the vicinity, and the spatial variation of the sky spectrum is also expected to be negligible. Nevertheless, the lower resolution *H*-band spectrum of Soifer et al. (1995) has a marginally detected blue wing to the [O III] lines, which may be Hβ.

Weak features near the predicted position of the He II 4686 line appears to be present, which might contribute to the unusual width of the apparent 4686-Å line in Soifer et al. (1995). However, none of these features is reliably detected, and none lies on any of the positions of $z = 2.286$ emission lines expected to be prominent (see, e.g., Section 4.4 below), which casts doubt on the reliability of the apparent detections. Soifer et al. (1995) quote a detection of He II 4686 Å at an O III/He II ratio of 23, much fainter than the limit ($\sim$5) placed in Fig. 5; this detection is confirmed, albeit tentatively, by Iwamuro et al. (1995).

The Hα line profile in our CGS4 *K*-band spectrum (Fig. 6) is clearly resolved into a broader resolved component, with width comparable to the UV emission lines, and a narrower unresolved component of Hα and [N II]. We fit the *K*-band spectrum using the **stsdas. fitting.ngauss** package with the background level as a free parameter, and with the following four Gaussians: first, three unresolved (FWHM 200 km s^{-1}) Gaussians to model the narrower Hα line and satellite [N II] 6548, 6584-Å lines, with the 6548-Å component constrained to have the same redshift and 1/3 the flux of the 6584-Å component; second, a further Gaussian with unconstrained amplitude, position and width. Although the broader component is a blend of the broader Hα and satellite [N II] lines, we model it as a single Gaussian for simplicity.

The results, displayed in Fig. 7, were very similar to a deblending with three Gaussians of unconstrained position and width, and further deblending models with alternative simplifying assumptions were attempted. In particular, the region between the narrower Hα and the narrower [N II]6584 lines was very poorly fitted in models without a broad excess, as might be expected from Fig. 7. The flux in this region is clear evidence for an additional component. From the variations in the narrower line flux between the models we estimate the flux errors in both the narrower Hα and [N II]6584-Å lines to be $\leq$30 per cent (Table 1). The flux from the broader Hα component (distinct from [N II]) is very poorly constrained.

Note that although the narrower Hα line is unresolved (FWHM less than $\sim$200 km s^{-1} at a resolving power of 1428), there is

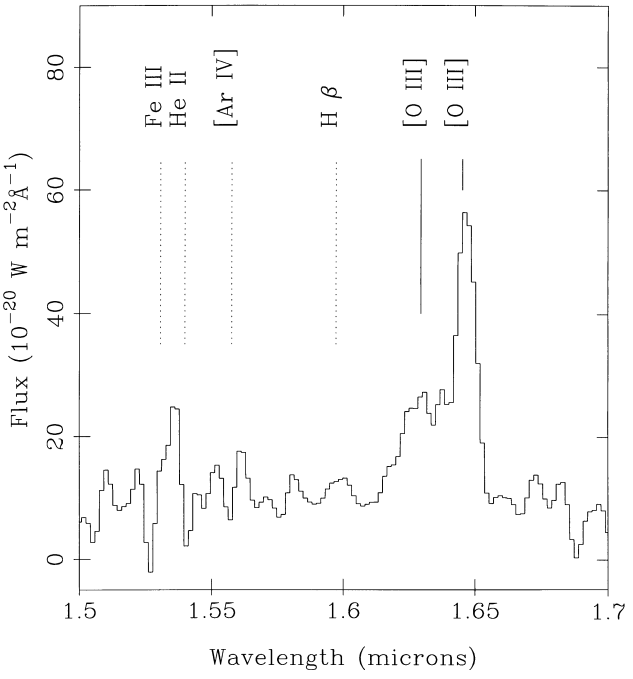

Figure 5. *H*-band spectrum of F10214 + 4724. The position of the [O III] doublet is marked, as are the predicted positions of other emission lines at $z = 2.286$.

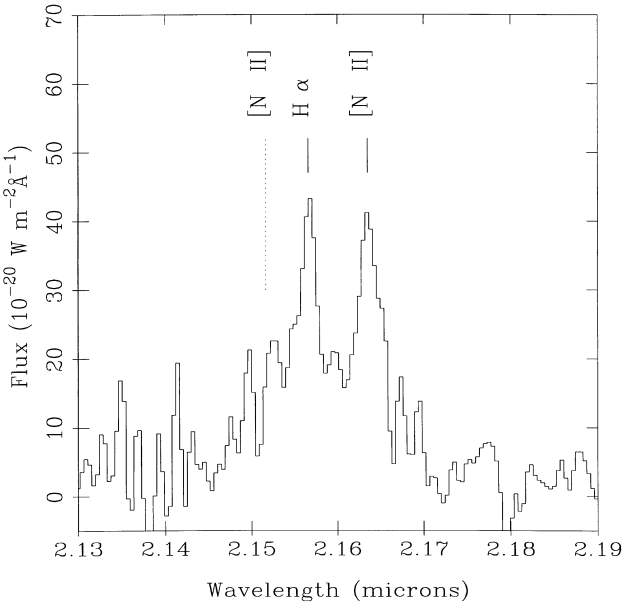

Figure 6. *K*-band spectrum of F10214 + 4724. The position of the narrower Hα and [N II] 6584-Å lines are marked assuming $z = 2.286$, as is the predicted position of the [N II] 6548-Å line. Note the clear broad base to these lines.

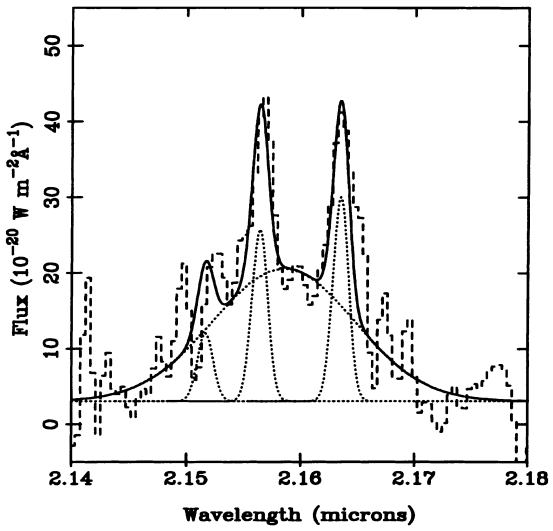

Figure 7. Fit to the *K*-band spectrum of F10214 + 4724 discussed in the text.

marginal evidence that the [N II] 6584-Å line is resolved. We found that at least some of the apparent excess on the [N II] line, if real, may be attributable to the broader [N II] component. If we assume that the satellite lines contribute 60 per cent of this flux, we obtain a broader Hα flux of 75 per cent of the total Hα. Note that the model does not imply the narrowest lines are Gaussian, but rather than the *K*-band spectrum must have at least one unresolved and at least one resolved component. This is exactly as expected for a hybrid starburst/AGN system.

To summarize, we find three distinct kinematic components in our new spectra of F10214 + 4724: first, a $\sim$1000 km s^{-1} component, present in Hα and in the UV lines which comes from the Seyfert 2 narrow-line region (NLR), as will be discussed further in Section 4; second, a < 200 km s^{-1} component, present in Hα, which we chose to associate with starburst activity, as will be discussed in Section 5; and, third, a 4000 km s^{-1} C III]1909 line which originates in a hidden Seyfert 1, or quasar, nucleus, as has been discussed by Goodrich et al. (1996).

4 THE SEYFERT 2 NARROW-LINE REGION

4.1 Resonant scattering of Lyman series lines

There is strong evidence for resonant scattering of the Lyα emission line: the profile of Lyα is double-peaked, and the peaks are symmetrically displaced about the predicted position of Lyα at $z = 2.286$ with equal flux (within the errors; Table 1). If the Lyα-emitting region is free of dust, then the velocity shift v of either Lyα peak from 1215.7 Å is given by

$$v = 195\left(\frac{N_{\rm H}}{10^{23}\ {\rm m}^{-2}}\right)^{1/3}\left(\frac{T}{10^4\ {\rm K}}\right)^{1/6}\ {\rm km\ s}^{-1} \qquad (1)$$

(Neufeld & McKee 1988), where $N_{\rm H}$ is the total atomic hydrogen column density to the source of the Lyα photons, and T is the gas temperature. The measured velocity separation of the peaks is $2\times\sim$560 km s^{-1}, yielding $N_{\rm H} = 2.5\times10^{25}$ m^{-2} for $T = 10^4$ K.

The total line-centre optical depth to the source of the Lyα photons is $\tau_{{\rm Ly}\alpha} \sim N_{\rm H}\times k_{{\rm Ly}\alpha}$, where $k_{{\rm Ly}\alpha}$ is the absorption cross-section to the line centre of Lyα. In the general case of photon absorption promoting an electron upwards in energy from level i to level j, the line-centre cross-section $k_{\rm l}$ is given by

$$k_{\rm l} = \frac{1}{4\pi\epsilon_0}\,\frac{\sqrt{\pi}e^2 f_{ij}}{mc\Delta\nu_D}, \qquad (2)$$

where f_{ij} is the oscillator strength for the transition, m and e are the electronic mass and charge, c is the speed of light, and ϵ_0 is the vacuum permittivity; $\Delta\nu_{\rm D} = (2kT/M_{\rm A}c^2)^{0.5}\times\nu_0$ is the Doppler width of the line with ν_0 the central frequency, k is the Boltzmann constant, and $M_{\rm A}$ is the atomic mass. In the case of the Lyα line, taking $T = 10^4$ K, these equations yield $k_{{\rm Ly}\alpha} = 5.8\times10^{-18}$ m^2, and thus $\tau_{{\rm Ly}\alpha} = 1.5\times10^8$.

Resonant scattering is extremely efficient at removing Lyβ photons even at moderate optical depths (e.g. Netzer 1975; Osterbrock 1989), in agreement with the null detection of Lyβ in F10214 + 4724. The strong influence of resonant scattering on the observed properties of the Lyman series lines is a major difference between the spectroscopic properties of F10214 + 4724 and NGC 1068. UV spectroscopy of the latter (Kriss et al. 1992b) shows a strong single-peaked Lyα line as well as Lyβ; the observed Lyβ/Lyα flux ratio of 0.12 implies $\tau_{{\rm Ly}\alpha} \lesssim 10$.

Is this neutral material within the NLR, or external, such as a damped Lyα system associated with the host galaxy? The QSO proximity effect (e.g. Giallongo et al. 1996) suggests that neutral material is often destroyed within the ionization cone. If the $N_{\rm H}$ is associated with the host, it need not cause damped absorption in F10214 + 4724 itself (countering the most obvious criticism), because the geometry would allow scattering into the line of sight. This neutral hydrogen could be intrinsic to the host, or could be the result of accretion of gas-rich dwarfs; neutral systems with column densities $\geq10^{25}$ m^{-2} are known to undergo a strong cosmological evolution which dominates the evolution in $\Omega_{\rm g}$ (Wolfe et al. 1995).

Can the $N_{\rm H}$ gas-to-dust ratio, derived from the Lyα strength, be used to resolve this? Lyα photons are conserved in resonant scattering, but the Lyα strength can be suppressed by dust absorption between scatterings. The predicted case B Lyα flux from our broader Hα flux implies a suppression factor of $< 10^2$, the limit assuming no [N II] 6548, 6584. In the damped Lyα models of Charlot & Fall (1991), a neutral screen with velocity dispersion 10 km s^{-1} and column density as derived above yields a Lyα suppression of $\sim10^4$, but if the gas-to-dust ratio is $\sim$4 times lower than the values typically inferred from the reddening of quasars with damped systems, this can be reconciled with our observed Lyα. The Lyα flux therefore cannot exclude the possibility of a damped system associated with the host. Alternatively, the same models predict a suppression $\sim10^{-1}$ for sources distributed throughout the $N_{\rm H}$ (for a velocity dispersion of 1000 km s^{-1} the suppression becomes only $\sim$0.75), and the authors argue that geometrical factors could reduce this to unity.

There are difficulties with resonant scattering within the NLR: the clouds in the nearer ionization cone suffer resonant scattering, but we nevertheless ought to have an unobscured view of the clouds in the more distant ionization cone. This contradicts, for example, the observed lack of Lyβ, but this could be explained by differential magnification of the nearer ionization cone, or selective obscuration of the more distant ionization cone, e.g., by the host galaxy.

We nevertheless favour models with at least some of the neutral column in the rear of the narrow-line clouds themselves, since the photoionization models below (Section 4.2) favour ionization-bounded clouds. Higher resolution *K*-band spectroscopy may resolve the AGN Hα from the satellite [N II] lines, and the inferred Lyα suppression may exclude the damped-system model. Spatially

resolved spectroscopy of F10214 + 4724 (while subject to the uncertainties in the projection to the source plane) may provide a further confirmation: diffuse Lyα could be used to trace any extended neutral hydrogen (Villar-Martin, Binette & Fosbury 1996), modulo the uncertainties in the projection to the source plane. The detection of non-resonance lines spatially coincident with any extended Lyα would rule out resonance scattering 'mirrors' and identify such emission with the AGN NLR or starburst knots.

4.2 Photoionization models

If we exclude the resonantly scattered Lyα, the marginally resolved doublet N v1240, 1243, and the blended emission lines (labelled in Table 1), then we find no correlation of ionization potential with emission linewidth. As a result, we may attempt to model the emission-line spectrum with constant-density, single-slab photoionization models, at least to first order.

We modelled the Seyfert 2 lines with the photoionization code CLOUDY (version 84.12, Ferland 1993), assuming for simplicity that the rest frame UV emission lines in F10214 + 4724 suffer zero extinction (Section 4.4). Unless otherwise stated, we used an AGN ionizing continuum as characterized by Matthews & Ferland (1987) with a break at 10 μm (see Ferland 1993). We considered hydrogen densities $8 \leq \log_{10} n \leq 16$, where n is the total hydrogen column density (i.e., molecular, neutral and ionized) in units of m^{-3}, and ionization parameters $-4 \leq \log_{10} U \leq 0$, where U is the dimensionless ratio of incident ionizing photons to hydrogen density, i.e., $U = \Phi(H)(nc)$. Here Φ is the surface flux of ionizing photons in $\mathrm{m}^{-2}\ \mathrm{s}^{-1}$, and c is the speed of light. The calculation was stopped at a column density of $10^{27}\ \mathrm{m}^{-2}$, or at a temperature of 4000 K, since below this temperature the emission-line flux is negligible. We used the default solar metallicity (see Ferland 1993), and CLOUDY assumes a plane-parallel geometry.

The He II:Lyα:O VI:C IV ratios are sensitive to the UV–soft X-ray continuum (e.g. Krolik & Kallman 1988), so are sensitive to the presence or absence of an active nucleus. A blackbody ionizing continuum at 40 000 K, resembling the continuum from the hottest OB stars, has severe difficulty in producing O VI1032, 1037 Å or Mg VI 1086 Å, due to the extremely high ionization potentials of O^{4+} and Mg^{4+} (0.11 and 0.14 keV respectively). The AGN ionizing continuum defined above had no difficulty in reproducing these lines. We are therefore confident that the $\sim$1000 km s^{-1} emission-line region is predominantly photoionized by the active nucleus.

None of the single-slab models provided an adequate fit to all the rest frame UV emission lines. We found that similar, but not identical, conditions ($\log_{10} n \sim 10$, $\log_{10} U \sim -1.5$) were implied by emission lines [Ne IV] 1602, He II 1640, N IV] 1486, N III] 1750, Ne V 3426, Ne III 3869. For example, the largest [Ne IV] 2424/He II 1640 ratio in our models was with a density and ionization parameter of $\log_{10} = 10$, $\log_{10} U = -1.4$. This underpredicts the O VI and Mg VI lines, as well as the N lines. However, the N III] 1486, 1750 and N V 1240 ratios are all consistent with $\log_{10} U \sim -1.25$; this self-consistency of the N lines suggests that the strength of the N 1240-Å line may be due mainly to an abundance effect, as also argued in the *IRAS*-detected Seyfert 2 galaxy NGC 3393 (Diaz et al. 1988), rather than due to differential magnification (Broadhurst & Lehár 1995). If so, this would further reduce the proportion of Hα in the broader component of Fig. 7.

This model reproduced the C IV:C III] ratio, but over-predicted their strength by a factor of $\sim$5. A low carbon abundance ($\sim$0.5$\times$ solar) might resolve the anomaly, perhaps caused by depletion on to dust grains. Much more problematic is the lack of an [O III] 1665-Å emission line, which in these conditions should have a flux $\sim$10 per cent of He II 1640 Å. There does not appear to be any simple solution; we note, however, that an identical problem was found by Kriss et al. (1992b) in NGC 1068, who argued that shock-heated gas would also produce the [O III] 1665 line.

Finally, we can use our limits on the density and ionization parameter to derive the sizes and masses of the NLR clouds. The clouds are ionization-bounded in the conditions we derived from the emission-line ratios, as is also conventionally assumed for AGN NLRs, and unlike, for example, the matter-bounded extended emission-line region models of Wilson, Walker & Thornley (1997). This supports our model for the resonant scattering (Section 4.1), and is also consistent with the presence of [O I] in the Keck spectrum (Soifer et al. 1995). Assuming that the absorbing column does indeed occur within the NLR clouds (assumed to be constant-density for simplicity), we obtain a characteristic size-scale of

$$S = N_{\mathrm{H}}/n_{\mathrm{H}} = 2.5 \times 10^{-2\pm0.5}\ \mathrm{pc}, \tag{3}$$

where the errors represent the acceptable range in the models, rather than, for example, Gaussian noise. The mean mass of the NLR clouds is given by

$$M = u \times n_{\mathrm{H}} \times S^3 = 1 \times 10^{-2\pm1}\ \mathrm{M}_{\odot}. \tag{4}$$

Unfortunately, it is not possible to derive a covering factor of volume filling factor without spatially resolved spectroscopy. Briefly, N clouds with covering factor C at mean distance D parsecs from a quasar with luminosity L are indistinguishable from N, $C/4$, $2D$, $4L$. We can, however, estimate the number of narrow-line clouds, and the total cloud mass contained in the NLR. Using CLOUDY, we find the emissivity of a single cloud of density $10^{10.5\pm0.5}\ \mathrm{m}^{-3}$ with ionization parameter $10^{-1.25\pm0.25}$; e.g., for the He II 1640 line $\epsilon = 10^{-2.4\pm0.7}\ \mathrm{W\ m}^{-2}$. For a magnification factor of $10\mathcal{M}_{10}$, our observed line flux implies the number of narrow-line clouds is

$$\begin{aligned} N &= (10^{-18}\ \mathrm{W\ m}^{-2} \times 4\pi D_L^2)/(4\pi\epsilon S^2 \times 10\mathcal{M}_{10}) \\ &= 1 \times 10^{7\pm1.4}\,\mathcal{M}_{10}^{-1} h_{50}^{-2}, \end{aligned} \tag{5}$$

where D_L is the luminosity distance to F10214 + 4724, given (assuming $\Omega_0 = 1$, $\Lambda = 0$, $H_0 = 50h_{50}$ km s^{-1} Mpc^{-1}) by

$$D_L = 0.04ch_{50}^{-1}(1 - (1 + 2.286)^{-0.5})(1 + 2.286). \tag{6}$$

(We also note that variations in S correlate with variations in the cloud emissivity, so the 'errors' do not simply add.) The inferred total mass of ionized gas within the narrow-line region is consistent with estimates in local AGN (e.g. Osterbrock 1993):

$$\begin{aligned} NM &= 10^{-18} 4\pi D_L^2 u n_{\mathrm{H}} S^3/(4\pi S^2 \epsilon 10\mathcal{M}_{10}) \\ &= N_{\mathrm{H}} \times 5 \times 10^{12\pm0.7}\mathrm{m}^2\,\mathcal{M}_{10}^{-1} h_{50}^{-2}\ \mathrm{kg} \\ &= 2 \times 10^{5\pm0.7}\,\mathcal{M}_{10}^{-1} h_{50}^{-2}\ \mathrm{M}_{\odot}. \end{aligned} \tag{7}$$

Our choice of He II, while free of metallicity effects, assumes negligible extinction (Section 4.4), which will be testable with higher quality infrared spectra. Note that if spatially resolved spectroscopy detects the emission-line counterimage, it may be possible to determine $\mathcal{M}_{10}$ independently of spatial structure in the *IRAS* galaxy. As a corollary to the covering factor calculation, one may then also obtain a robust estimate of the luminosity of the obscured quasar (Goodrich et al. 1996).

4.3 Optically thick O VI emission

The resonant O VI 1034, N V 1240 and C IV 1549 lines are doublets in

the isoelectronic lithium sequence. If such lines emanate from a region which is optically thin to resonant scattering, then their doublet line ratios are given by the ratio of the statistical weights of the upper levels, i.e., 2:1 with the lower wavelength line of the doublet the brighter. However, in optically thick regions, photon trapping and collision de-excitation can cause the levels to thermalize so that the flux ratio approaches ∼1:1; this thermalization occurs only at higher values of optical depth and electron density n_e, namely when $n_e\tau_0 \gtrsim 10^{22}$ m^{-3} (Hamann et al. 1995). A doublet ratio of 1:1 therefore implies extreme densities and/or optical depths.

The O VI 1031.9, 1037.6 doublet in F10214 + 4724 is clearly resolved (Fig. 4), and its flux ratio 1:1 suggests line thermalization. We first consider whether this ratio is strongly influenced by blanketing by the Lyα forest lines – both a simple empirical test and a brief analytical argument suggest that it is not. The test involved fitting low-order polynomials to the UV continuum longward of Lyα, and extrapolating these fits to shorter wavelengths to estimate the level of line blanketing. We then superimposed a model 2:1 doublet at several positions on this absorption spectrum, and found it impossible to obtain an apparent 1:1 ratio. This is in good agreement with the following analytical argument. The number of Lyα forest lines per unit redshift per unit restframe equivalent width is well fitted by an expression of the form

$$\frac{\mathrm{d}^2N}{\mathrm{d}z\mathrm{d}W} = \frac{A_0}{W^*}(1+z)^\gamma \exp\left(-\frac{W}{W^*}\right), \quad (8)$$

where $\gamma \simeq 1.89$, $W^* \simeq 0.27$ Å and $A_0 \simeq 10$ (e.g. Bechtold 1994). By integrating this over the redshift range 1.770 to 1.792 (i.e., in the neighbourhood of the doublet and exactly encompassing the width of either line of the doublet), and further integrating dN/dW, it can be shown that a maximum of two Lyα forest lines are expected to lie on the position of one O VI line. For a 2:1 doublet to be suppressed to 1:1, the line blanketing over the shorter wavelength line must be approximately a factor of 2 (in addition to the mean blanketing); the probability of this occurring is negligibly small, a conclusion which is insensitive to the uncertainties in γ, W^* and A_0.

This seems to imply that the O VI-emitting region in F10214 + 4724 is both optically thick ($\tau_{\mathrm{O\,VI}} \gg 1$) and dense enough for the doublet to have become thermalized, i.e., $n_e\tau_{\mathrm{O\,VI}} \gtrsim 10^{22}$ m^{-3}. We will next show that the optical depth $\tau_{\mathrm{O\,VI}}$ is unlikely to exceed 10^6, resulting in apparent BLR-like conditions for the narrow O VI-emitting region.

The latest release of CLOUDY (version 90.03a, Ferland 1996) incorporates the O VI 1032, 1037-Å doublet lines separately, so we used this code to explore the doublet ratios and O VI optical depths for a wide range of physical conditions. We used the same AGN ionizing continuum, metallicity and stopping conditions as above. The results are shown in Fig. 8. We find that the 1:1 ratio, also where the $n_e\tau_0 \gtrsim 10^{22}$ m^{-3} limit applies, is possible only with hydrogen densities in excess of $n_H \simeq 10^{17}$ m^{-3}. This conclusion was found to apply equally to $N_H = 10^{26}$ m^{-2} column and/or $Z = 10$ Z$_\odot$ metallicity gas. Such a high value of n_H is characteristic of the BLRs of AGN (e.g. Ferland et al. 1992) rather than the lower values ($n_e \sim 10^{11}$ m^{-3}) found in classical NLRs.

Such a radical conclusion can be avoided, albeit with some fine-tuning, by considering the Lyβ resonant absorption. This absorption is likely to be saturated, so the O VI doublet may lie inside its damping wings. Using the N_H value derived above, we obtain an optical depth of about 0.3 for the 1032-Å line, and 0.09 for the 1038-Å line (i.e., a factor ∼3.6). To obtain a 1:1 ratio from 2:1, one needs an optical depth of around 1 to the 1032-Å line, close to the

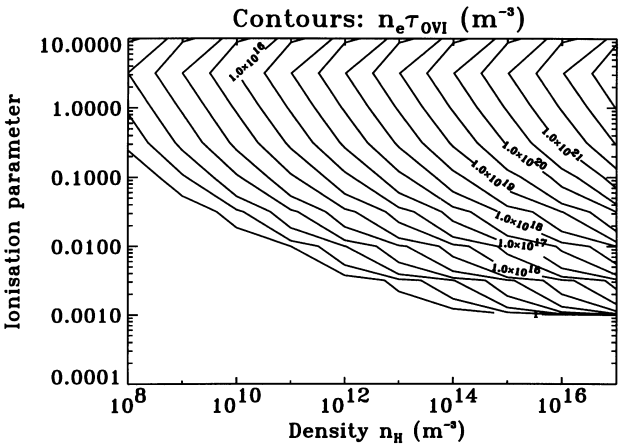

Figure 8. Results of the photoionization model discussed in the text. The contours show the product of the n_p-weighted average electron density and O VI 1032 + 1037-Å optical depth, $n_e \times \tau_{\mathrm{O\,VI}}$, as functions of ionization parameter and density. (Almost identical results were obtained replacing this n_e with the innermost zone electron density, the outermost, or the total hydrogen density.) The contours are spaced logarithmically in steps of 0.5. Only where $n_e \times \tau_{\mathrm{O\,VI}} \gtrsim 10^{22}$ m^{-3} does the O VI doublet form a 1:1 ratio.

estimate from the observed N_H. This explanation avoids the high densities, but is sensitive to the assumed neutral column, and furthermore takes no account of geometrical effects (Villar-Martin et al. 1996).

Inspection of the UV spectrum of NGC 1068 (Kriss et al. 1992b) suggests that the O VI doublet is again in a ∼1 : 1 ratio. However, there is no evidence of resonant scattering in this object.

4.4 Reddening of the Seyfert 2 nucleus

We can place limits on the extinction in the observed UV from the He II 1640 Å/He II 1086 Å ratio, which in the absence of reddening is predicted to be 7 (e.g. Seaton 1978). Although the signal-to-noise ratio shortward of Lyα in Fig. 4 is poor, and despite possible blanketing by Lyα forest lines, the He II 1086-Å line is marginally detected at (∼7 ± 50 per cent)$^{-1}$ times the flux of the 1640-Å counterpart. If real, this suggests an extinction of between zero and 0.75 mag around 1200 Å in the rest frame of F10214 + 4724 (i.e., $A_V < 0.2$), or 2600 Å in that of the lens (i.e., $A_V < 0.4$). We can also obtain a rough extinction estimate from the Hα:He II 1640 Å ratio, predicted to be about 2.3 in our solar-metallicity models above. We find (Hα + [N II]):He II = 3.8, consistent with an Hα:N II ratio resembling, e.g., NGC 1068 (e.g. Bland-Hawthorn, Sokolowski & Cecil 1991) and zero extinction.

Comparison of the H-band detection of the He II 4686-Å line (e.g. Soifer et al. 1995) with the 1640-Å line suggests extinctions $A_V \sim 1.3$. However, our photoionization models above found the Fe II 4658-Å and/or Ar IV 4720-Å lines can contribute up to 3 times the flux of the He II 4686-Å line in densities of 10^{10}–10^{12} m^{-3}, not unreasonable for AGN NRLs. Moreover, the Soifer et al. H-band spectrum has very low spectral resolution, and the He II 4686-Å line flux must be treated with some caution.

This low reddening in the rest frame UV is in marked contrast to the high ($A_V \geq 5$) rest frame optical extinction derived from Balmer decrements (e.g. Soifer et al. 1995), which led several authors to infer that at least two physically distinct regions contribute to the observed emission-line spectrum (e.g. Elston et al. 1994; Soifer et al. 1995). The limit on the Balmer decrement of Hα:H$\beta \geq 20$ reported by Elston et al. (1994) is at least in part resolved by our

K-band spectrum. The narrower Hα component contributes $\sim$25 per cent of the total Hα flux; furthermore, our total Hα flux is $\sim$25 per cent lower than that reported by Elston et al., although this is within their stated photometric errors. However, this still yields $A_V > 4$ in the frame of F10214 + 4724, or $A_V > 6$ in that of the lens. (Any < 200 km s^{-1} Hβ leads to an even higher A_V.) Alternatively, if we assume that the Iwamuro et al. (1995) Hβ detection is correct, the data are consistent with zero extinction. Further near-infrared spectroscopy is required to resolve this issue. We conclude that as yet there is no conclusive evidence for any significant reddening of the Seyfert 2 nucleus.

5 STARBURST PROPERTIES

Our limit on the width of the narrowest Hα component in F10214 + 4724 is suggestive of a star-forming region, as has previously been suggested by Kroker et al. (1996). Moreover, the fluxes of the [O I] 6300-Å and [S II] 6724-Å lines (Soifer et al. 1995) relative to the narrowest Hα component are similar to both those seen in spectra of local starburst galaxies (e.g. De Robertis & Shaw 1988) and in high-luminosity *IRAS* galaxies (e.g. Leech et al. 1989). We can obtain an estimate of the star formation rate R from the narrower Hα line flux S, using the following expression adapted from Kennicutt (1983):

$$R(z = 2.286) = \frac{S(\mathrm{H}\alpha)h_{50}^{-2}}{3 \times 10^{-21}\ \mathrm{W\ m^{-2}}}\ \mathrm{M_\odot\ yr^{-1}}. \quad (9)$$

We assume a Hubble constant of $H_0 = 50\ h_{50}$ km s^{-1} Mpc^{-1} with $\Omega_0 = 1$, $\Omega_\Lambda = 0$. If we assume that the starburst region undergoes a net gravitational magnification of $\mathcal{M} \lesssim 10$ (Downes et al. 1995; Graham & Liu 1995; Green & Rowan-Robinson 1996), and that aperture corrections are negligible, we obtain a star formation rate of $\gtrsim 20 h_{50}^{-2}$ M$_\odot$ per year. This corresponds to a starburst luminosity of $\gtrsim 2.6 \times 10^{11} h_{50}^{-2}$ L$_\odot$ (e.g. Moorwood 1996), i.e., $\sim$0.5 per cent of the magnification-corrected bolometric power output.

Reddening by intervening dust would further increase this estimate of the star formation rate. Radiative transfer models of F10214 + 4724 (Green & Rowan-Robinson 1996) suggest a much larger starburst bolometric fraction of $\sim$0.2–0.4, with a high starburst UV optical depth of $\tau_{\mathrm{UV}} \sim 800$, i.e., an $A_V \sim 160$. Assuming that this dust is well mixed with the Hα-emitting gas (e.g. Thronson et al. 1990), the extinction and star formation rate is quite consistent with our observed narrow Hα flux, which for this A_V yields a starburst bolometric fraction of $\sim$0.5. In both NGC 1068 (Green & Rown-Robinson 1996) and F10214 + 4724, the starburst and active nuclei appear to make comparable contributions to the bolometric power output.

6 CONCLUDING REMARKS

The presence of the optically thick O VI 1032, 1037-Å doublet appears at face value to imply extremely high densities for narrow emission-line gas, $n_{\mathrm{H}} \gtrsim 10^{17}$ m^{-3}. However, we argue that it is more easily attributable to the Lyβ damping wings of resonant scattering material, probably within the AGN NLR. Differential magnification appears to play a significant role in the emission-line spectrum of F10214 + 4724, in which we identify three distinct kinematic components: quasar broad lines ($\sim$4000 km s^{-1}), Seyfert 2 narrow lines ($\sim$1000 km s^{-1}) and a starburst component ($\lesssim$200 km s^{-1}). The density, ionization parameter, number and total mass of Seyfert 2 narrow-line clouds all resemble local Seyferts, and our interpretation of the resonant scattering agrees with that of Villar-Martin et al. (1996) for high-redshift radio galaxies. The flux from the narrowest Hα component is in excellent agreement with radiative transfer models which comprise similar quasar and starburst bolometric contributions.

ACKNOWLEDGMENTS

We thank Carlos Martin for assisting the observations. The WHT is operated on the island of La Palma by the Royal Greenwich Observatory in the Spanish Observatorio del Roque de los Muchachos of the Instituto de Astrofisica de Canarias. We thank Steve Eales for performing the GASP astrometry of the F10214 + 4724 field, and for (unwittingly) contributing observing time to the project. We also thank Tony Lynas-Gray, Geoff Smith and Steve Warren for useful discussions.

REFERENCES

Adams T., 1972, MNRAS, 174, 439
Antonucci R., Hurt T., Miller J., 1994, ApJ, 430, 210
Barvainis R., Tacconi L., Antonucci R., Allion D., Coleman P., 1994, Nat, 371, 586
Bechtold J., 1994, ApJS, 91, 1
Blandford R. D., Kochanek C. S., 1987, ApJ, 321, 658
Bland-Hawthorn J., Sokolowski J., Cecil G., 1991, ApJ, 375, 78
Broadhurst T., Lehár J., 1995, ApJ, 450, L41
Bruzual A. G., Charlot S., 1993, ApJ, 405, 538
Charlot S., Fall S. M., 1991, ApJ, 378, 471
Clements D., van der Werf P., Krabbe A., Blietz M., Genzel R., Ward M., 1993, MNRAS, 262, 23P
Close L. M., Hall, P. B., Liu C. T., Hége E. K., 1995, ApJ, 452, L9
Davidson K., Netzer H., 1979, Rev. Mod. Phys., 51, 715
De Robertis M. M., Shaw R. A., 1988, ApJ, 329, 629
Diaz A. I., Prieto M. A., Wamsteker W., 1988, A&A, 195, 53
Downes D., Radford S. J. E., Greve A., Thum C., Solomon P. M., Wink J. E., 1992, ApJ, 398, L25
Downes D., Solomon P. M., Radford S. J. E., 1995, ApJ, 453, 65
Dunlop J. S., Hughes D. H., Rawlings S., Eales S. A., Ward M. J., 1994, Nat, 370, 347
Eisenhardt P. R., Armus L., Hogg D. W., Soifer B. T., Neugebauer G., Werner M. W., 1996, ApJ, 461, 72
Elston R., McCarthy P. J., Eisenhardt P., Dickinson M., Spinrad H., Januzzi B. T., Maloney P., 1994, AJ, 107, 910
Ferland G. J., 1993, University of Kentucky Department of Physics and Astronomy Internal Report
Ferland G. J., 1996, Hazy, a Brief Introduction to Cloudy. University of Kentucky Department of Physics and Astronomy Internal Report
Ferland G. S., Peterson B. M., Horne K., Welsh, W. F., Nahar S. N., 1992, ApJ, 387, 95
Giallongo E., Cristiani S., D'Odorico S., Fontana A., Savaglio S., 1996, ApJ, 466, 46
Goodrich R., Miller J., Martel A., Cohen M., Tran H., 1996, ApJ, 456, L9
Graham J. R., Liu M. C., 1995, ApJ, 449, L29
Green S. M., Rowan-Robinson M., 1996, MNRAS, 279, 884
Hamann F., Shields J. C., Ferland G. J., Korista K. T., 1995, ApJ, 454, 688
Hines D. C., Schmidt G. D., Cutri R. M., Low F. J., 1995, ApJ, 450, L1
Hughes D. H., Dunlop J. S., Rawlings S., 1997, MNRAS, 289, 766
Iwamuro F., Maihara T., Tsukamoto H., Oya S., Hall D. B., Cowie L. L., 1995, PASJ, 47, 265
Jannuzi B. T., Elston R., Schmidt G. D., Smith P. S., Stockman H. S., 1994, ApJ, 429, L49
Kennicutt R. C., Jr., 1983, ApJ, 272, 54
Kennicutt R. C., Jr., Tamblyn P., Congdon C. E., 1994, ApJ, 435, 22
Kriss G. A. et al., 1992a, ApJ, 392, 485
Kriss G. A. et al., 1992b, ApJ, 394, L37
Kroker H., Genzel R., Krabbe A., Tacconi-Garman L. E., Tecza M., Thatte N., 1996, ApJ, 463, L55

Krolik J. H., Kallman T. R., 1988, ApJ, 324, 714
Lacy M., Rawlings S., 1994, MNRAS, 270, 431
Laor A. et al., 1994, ApJ, 420, 110
Lawrence A. et al., 1993, MNRAS, 260, 268
Lawrence A., Rigopoulou D., Rowan-Robinson M., McMahon R. G., Broadhurst T., Lonsdale C. J., 1994, MNRAS, 266, L41
Leech K. J., Penston M. V., Terlevich R., Lawrence A., Rowan-Robinson M., Crawford C., 1989, MNRAS, 240, 349
Matthews W. G., Ferland G. J., 1987, ApJ, 323, 456
Matthews K. et al., 1994, ApJ, 420, L13
Mendoza C., 1983, in Planetary nebulae: Proc. Symp. London. Reidel, Dordrecht, p. 143
Moorwood A. F. M., 1996, Space Sci. Rev., 77, 303
Mountain C. M., Robertson D. J., Lee T. J., Wade R., 1990, in Crawford D. L., ed., Instrumentation in Astronomy VII. Proc. SPIE, 1235, 25
Nelson C. H., Whittle M., 1996, ApJ, 465, 96
Netzer H., 1975, MNRAS, 171, 395
Neufeld D. A., McKee C. F., 1988, ApJ, 331, L87
Osterbrock D. E., 1989, Astrophysics of Gaseous Nebulae and Active Galactic Nuclei. University Science Publications, Mill Valley, CA, USA
Osterbrock D. E., 1993, ApJ, 404, 551
Radford S. J. E., Brown R. L., Vanden Bout P. A., 1993, A&A, 271, L21
Ramsay S. K., Mountain C. M., Geballe T. R., 1992, MNRAS, 259, 751
Rowan-Robinson M. et al., 1991, Nat, 351, 719
Rowan-Robinson M. et al., 1993, MNRAS, 261, 513
Scoville N. Z., Yun M. S., Brown R. L., Vanden Bout P. A., 1995, ApJ, 449, L109
Seaton M. J., 1978, MNRAS, 185, 5P
Serjeant S., Lacy M., Rawlings S., King L. J., Clements D. L., 1995, MNRAS, 276, L31
Snidjers M. A. J., Netzer H., Boksenberg A., 1986, MNRAS, 222, 549
Soifer B. T., Neugebauer G., Matthews K., Lawrence C., Mazzarella J., 1992, ApJ, 399, L55
Soifer B. T., Cohen L., Armus K., Matthews G., Neugebauer G., Oke J. B., 1995, ApJ, 443, L65
Solomon P. M., Downes D., Radford S. J. E., 1992, ApJ, 398, L29
Thronson H. A., Majewski S., Descartes L., Hereld M., 1990, ApJ, 364, 456
Trentham N., 1995, MNRAS, 277, 616
Villar-Martin M., Binette L., Fosbury R. A. E., 1996, A&A, 312, 751
Warren S., Hewett P., Osmer P., 1994, ApJ, 421, 412
Wills B. J., Netzer H., Wills D., 1980, ApJ, 242, L1
Wilson C. D., Walker C. E., Thornley M. D., 1997, ApJ, 482, 131
Wolfe A. M., Lanzetta K. M., Foltz C. B., Chaffee F. H., 1995, ApJ, 454, 698

APPENDIX A: COMPANION GALAXIES

Fig. A1 shows the spectrum of a galaxy ~19 arcsec south-west of the *IRAS* galaxy, which fortuitously lay on the slit in our WHT observations. The feature at around 5510 Å is probably a low-energy cosmic ray event, but the emission lines at 7155 Å and (marginally) at 5323 Å appear to be real, since they occur in the spectra on both nights. Cross-correlating this spectrum with old galaxy models (a 1-Gyr burst aged by 6×10^8 yr to 1 Gyr) from Bruzual & Charlot (1993) yields two redshift estimates, 0.428 and 0.476 (both ± ~ 5 per cent). We prefer the former, which identifies the weak emission features as [O II]3727 and [O III]5007. Close et al. (1995) report a similar redshift, 0.429 ± 0.002 for a further galaxy ~23 arcsec south-west of the *IRAS* galaxy. The UV upturn in Fig. A1 may indicate a recent starburst, as expected perhaps if the galaxies are tidally interacting. However, there could be a slight systematic error in the redshift of the Close et al. companion. The emission-line wavelengths in their spectrum of F10214 + 4724 are offset by a factor of ~0.99 compared to other published spectra (e.g. Rowan-Robinson et al. 1993; Goodrich et al. 1996), and the residuals from the 5577-Å sky feature also appear to be offset by a similar amount.

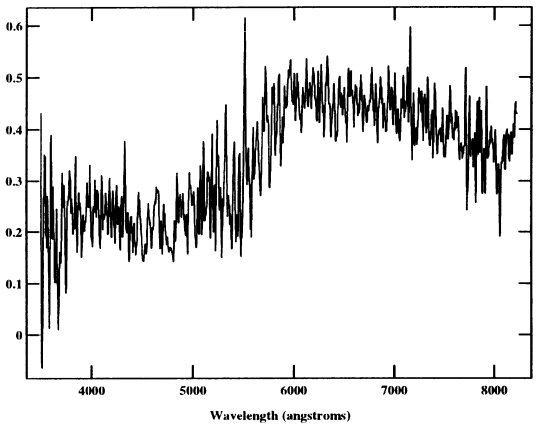

Figure A1. Serendipitous galaxy ~19 arcsec south-west of F10214 + 4724. The flux has units 10^{-20} W m^{-2} Å^{-1}, and the spectrum is extracted with a full-width zero-intensity aperture.

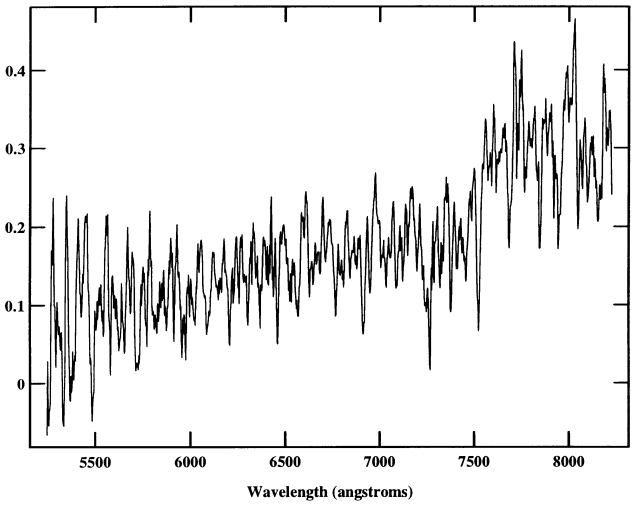

Figure A2. The sum of the spectra of sources 2 and 3 (in the notation of Matthews et al. 1994). These spectra were extracted with 3-pixel (~1.1 arcsec) apertures, differing slightly from the method of Serjeant et al. 1995, though with very little quantitative difference. Source 2 is corrected for contamination by the *IRAS* galaxy by subtracting a spectrum of F10214 + 4724 scaled by the strength of the C III]1909 line. The sum has been smoothed with a 5-pixel (~14-Å) boxcar. The flux has units 10^{-20} W m^{-2} Å^{-1}.

The tentative lens redshift of $z \simeq 0.90$ (Serjeant et al. 1995) is consistent with both its velocity dispersion (e.g. Broadhurst & Lehár 1995) and surface brightness profile (Eisenhardt et al. 1996). Further support for this lens redshift comes from Fig. A2, in which the spectra of sources 2 and 3 (Serjeant et al. 1995) are summed. Source 2 is the lensing galaxy, and source 3 is the companion ~3.3 arcsec north-east of the *IRAS* galaxy, in the notation of Matthews et al. (1994). If the galaxies are indeed associated, as suggested by their similar spectral energy distributions and tentative 4000-Å breaks (Serjeant et al. 1995), as well as by hints of tidal interaction in *HST* imaging (Eisenhardt et al. 1996), then the summed spectrum should show a $\sim\sqrt{2}$ improvement in signal-to-noise ratio, which is indeed the case in Fig. A2.

Several groups have also noted the slight over-density of galaxies in the vicinity of F10214 + 4724. The discovery of a Mg II absorber

in the Keck spectrum at $z = 1.316$ (Goodrich et al. 1996), and the possibly associated pair at $z \simeq 0.4$, implies that several physically independent systems, at a variety of redshifts, contribute to the overdensity in the field.

APPENDIX B: THE MYSTERY LINE AT 2067 Å

In this appendix we summarize our attempts to identify the line at 2067 Å in the rest frame spectrum of F10214 + 4724. We have made an extensive literature search, and investigated synthetic spectra generated by the CLOUDY photoionization code over wide ranges of ionization parameter and abundances (version 84.12, Ferland 1993; see also Section 4.2). This led to only two possible identifications for this line. The first of these is the resonant boron B III 2068 doublet, the next resonance line in the lithium isoelectronic sequence below the bright O VI, N V and C IV lines. The tiny cosmic abundance of boron means that this line is predicted to be immeasurably faint, and we therefore reject this possibility. The second possibility is the forbidden [Na V] 2067.9/2069.8 doublet (Mendoza 1983) – a line which is not found in the CLOUDY version 84.12 output.

To determine whether the [Na V] 2067.9/2069.8 doublet is a plausible identification for the mystery line, we have compared its predicted strength with that of [Ne IV] 2422.5/2425.1. These two pairs of collisionally excited lines arise from electronic transitions within adjacent ions in the nitrogen isoelectronic sequence. In the low-density limit the ratio of the cooling rates in these doublets is given by

$$\frac{L_{2069}}{L_{2424}} = \frac{n_{\mathrm{Na\,V}}}{n_{\mathrm{Ne\,IV}}} \times \frac{\mathrm{e}^{-\chi_{2069}/kT}}{\mathrm{e}^{-\chi_{2424}/kT}} \times \frac{\Omega_{2069}}{\Omega_{2424}} \times \frac{2424}{2069} \tag{10}$$

(Osterbrock 1989), where χ_λ is the excitation potential of the upper energy level(s), and Ω_λ is the effective collision strength (see Mendoza 1983).

Adopting $T = 10^4$ K and solar abundances, and assuming that the fraction of Na in the Na^{4+} state is similar to the fraction of Ne in the Ne^{3+} state, the value of this ratio is ≈0.005. The measured ratio is ≈0.23, so at first sight the putative [Na V] 2067.9/2069.8 doublet would need to be anomalously strong. However, at higher densities, collisional de-excitation may become important. The critical densities for collisional de-excitation n_{crit} are $\sim 10^{11}$ and $\sim 10^{12}$ m^{-3} for the lower wavelength lines in the Ne and Na doublets respectively (in each case the higher wavelength doublet line has an order of magnitude lower n_{crit} than its partner). Given the weakness of the [O II]3727 line, with $n_{\mathrm{crit}} \sim 10^{10}$ m^{-3} in F10214 + 4724, and the strengths of the [O III]4959/5007 line and forbidden neon lines (with $n_{\mathrm{crit}} \gtrsim 10^{12}$ m^{-3}) (Soifer et al. 1995), it is certainly feasible that collisional de-excitation can account for the strength of the putative [Na V] doublet with respect to the [Ne IV] doublet.

We conclude that the [Na V]2067.9/2069.8 doublet is a probable identification for the mystery line in the spectrum of F10214 + 4724 and, by analogy, in NGC 1068 and other active galaxies.